Supporting Information

Development of a cysteine-conjugatable disulfide FRET probe: Influence of Charge on Linker Cleavage and Payload Trafficking for an anti-HER2 antibody conjugate

Suzie J. Scales, Siao Ping Tsai, Neelie Zacharias, Josefa dela Cruz-Chuh, Gordy Bullen, Erick Velasquez, Julie Chang, Elise Bruguera, Katherine R. Kozak, Jack Sadowsky*

Research & Early Development, Genentech, Inc., 1 DNA Way, South San Francisco, CA 94080

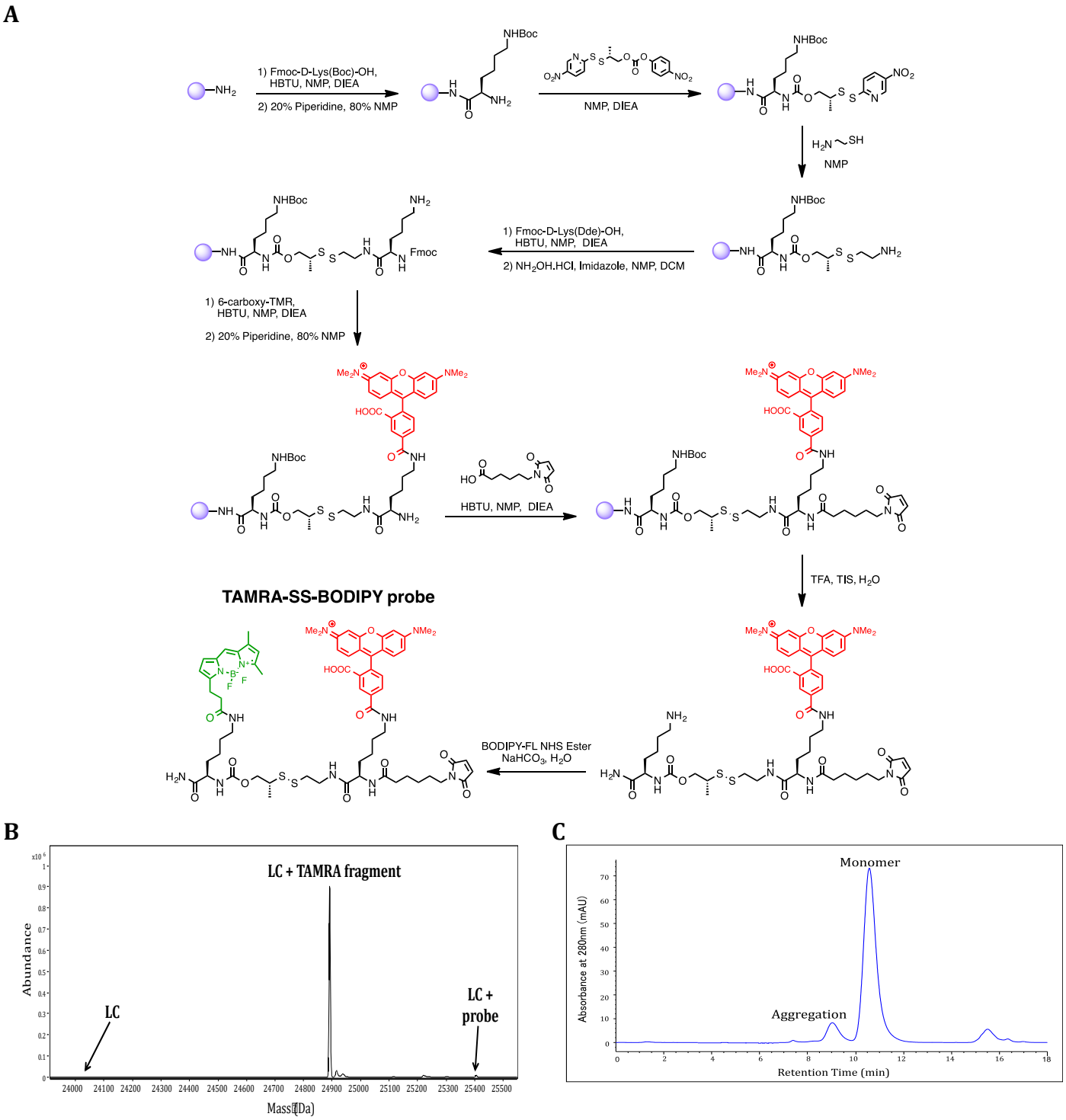

Figure S1. Analytical characterization of probe **Her2-SS**. (A) Solid-phase synthesis of the **TAMRA-SS-BODIPY** disulfide probe (see Materials and Methods for details). (B) Deconvoluted mass spectrum for **Her2-SS** probe conjugate treated with 10 mM DTT at 37°C for ~15 minutes showing expected masses for light chain (LC), light chain conjugated to the intact probe (LC + probe) and light chain conjugated to the TAMRA portion remaining upon disulfide cleavage (LC + TAMRA fragment). (C) Size-exclusion chromatogram (SEC) for **Her2-SS** showing ~89% of the preparation is monomeric, the remainder being of higher molecular weight (aggregate).

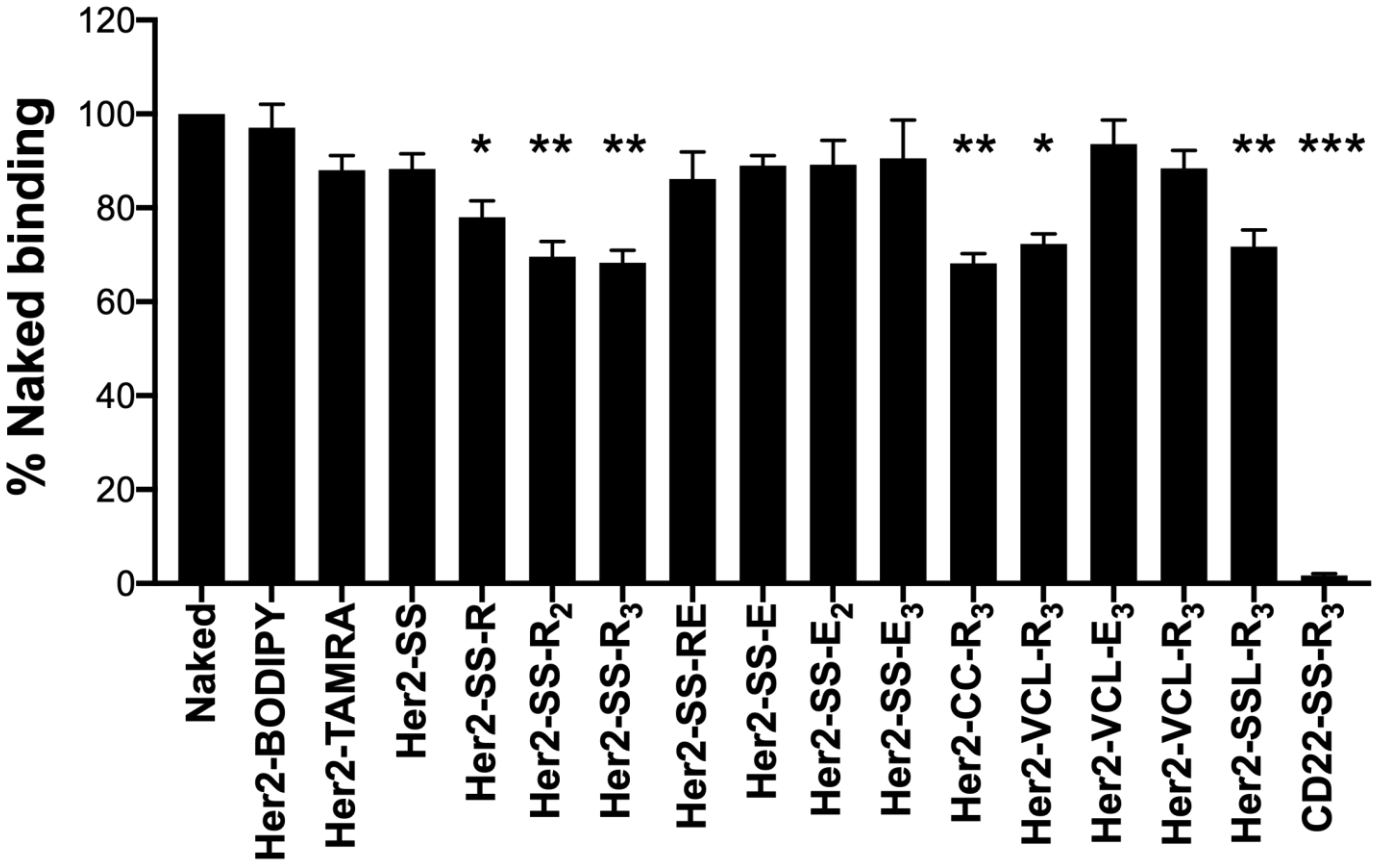

Figure S2. All Her2 (7C2 antibody) conjugates bind to MCF-7/HER2 cells. MCF-7/HER2 cells were incubated on ice with a saturating concentration (5 μg/ml) of the indicated **Her2** conjugates, unconjugated 7C2 anti-HER2^{K149C} ("naked" antibody), or non-binding control **CD22-SS-R$_3$** and detected with 2 μg/ml Alexa 647-anti-human Fc secondary antibodies. Mean fluorescence intensities were calculated as a percentage of unconjugated anti-HER2^{K149C} binding and the means and standard deviations of 3 independent duplicate experiments are plotted. All conjugates bound well to MCF-7/HER2 cells, although the TAMRA-containing conjugates, especially those also containing dArg, were either less efficiently bound or less well detected with the anti-Fc secondary. Almost identical results were obtained using Alexa 647-anti heavy and light chains as a secondary antibody (data not shown). * $p < 0.05$, ** $p < 0.01$, *** $p < 0.001$ versus naked 7C2 by t-test.

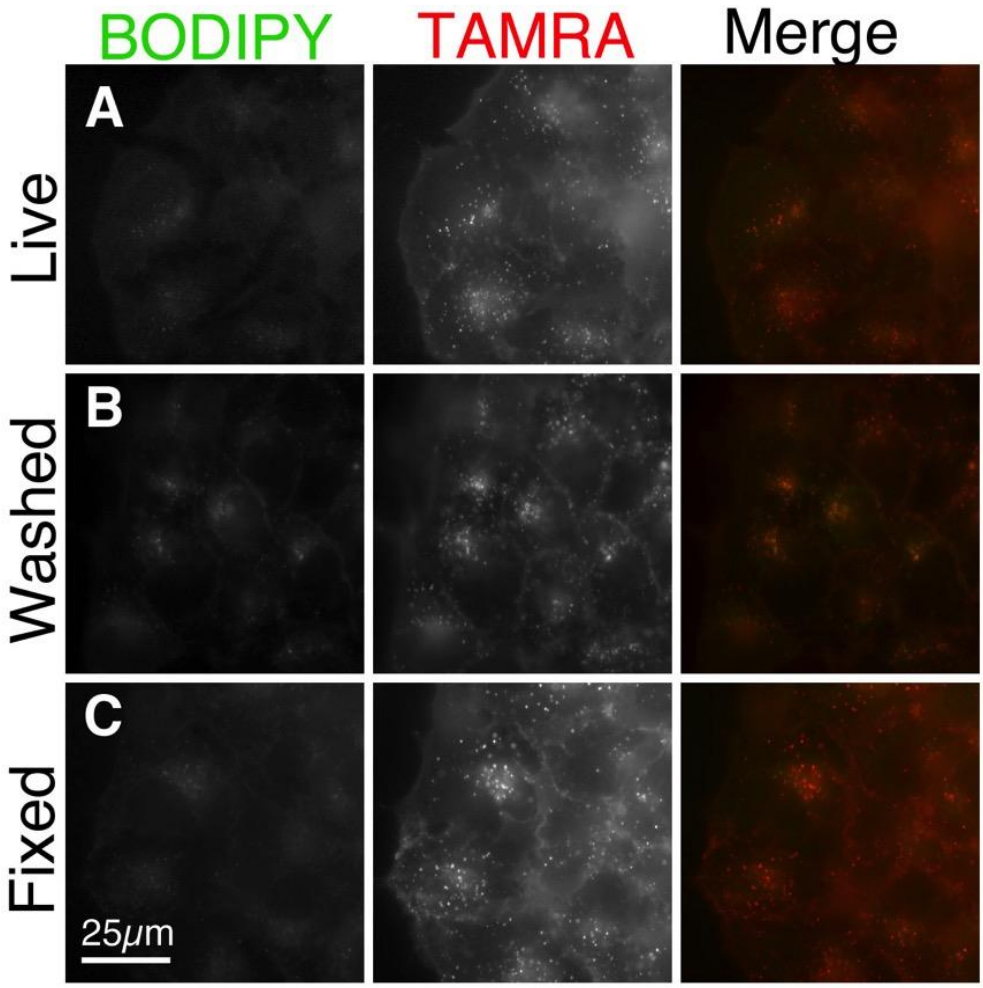

Figure S3. Her2-SS gives similar signals in live and fixed cells. Cells were incubated with **Her2-SS** as described under **Figure 2B**, except they were first imaged live (A), then washed and imaged live again (B), then PFA fixed and re-imaged (C). In all cases there was negligible BODIPY signal (green, left) in the cells compared to TAMRA (red, center). Merged images are shown on the right. Scale bar is 25 μm.

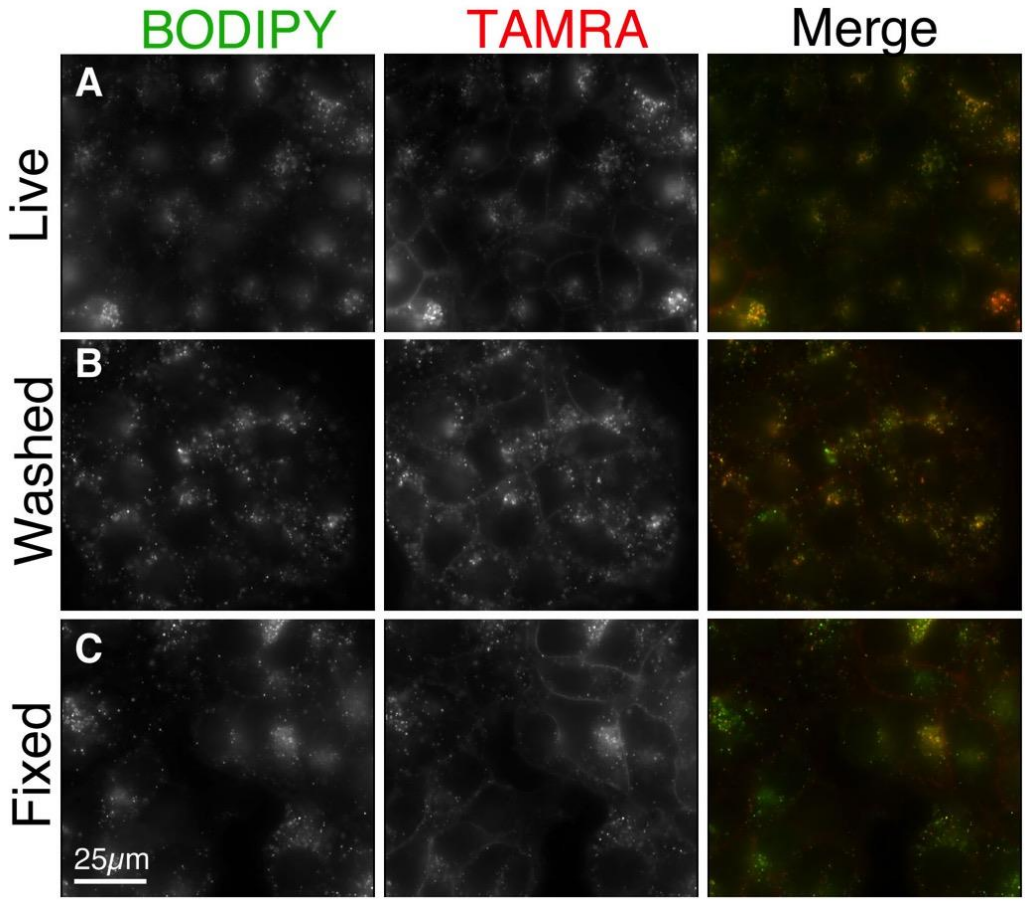

Figure S4. Her2-SS-R$_3$ gives similar signals in live and fixed cells. MCF-7/HER2 cells were incubated with **Her2-SS-R$_3$** as in **Figure 5**, except they were first imaged live (A), then washed and imaged live again (B), then PFA fixed and re-imaged (C). In all cases BODIPY signal (green, left) was seen intracellularly and colocalized with intracellular (but not cell surface) TAMRA (red, center). Merged images are shown on the right. Scale bar is 25 μm.

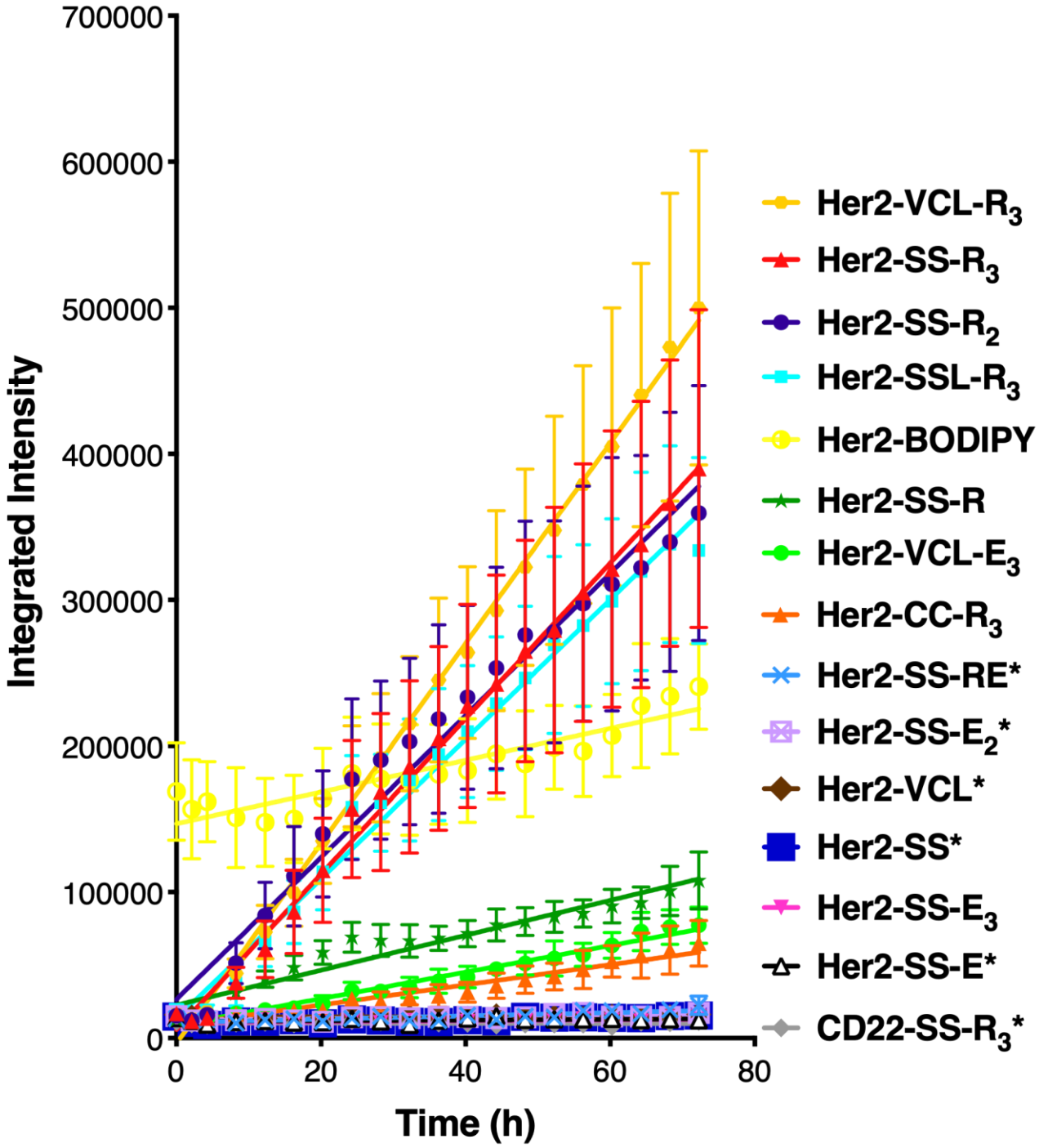

Figure S5. Time-course cleavage of all Her2 probes in live SK-BR-3 cells. All the conjugates were tested in a single experiment as in **Figure 7C**, with means and SDs of 4 replicates plotted for comparison. Conjugates are listed from top to bottom in decreasing order of fluorescence obtained, including those marked with asterisks at the bottom of the graph that did not yield much or any meaningful fluorescence. Note that the **R2** and **R3** probes actually achieved higher integrated fluorescence intensity than **Her2-BODIPY** maximal fluorescence control, strongly implying superior cellular retention by positive charges. Note also that the negatively charged **E3** probe is detectable with the VCL (**Her2-VCL-E3**) but not disulfide (**Her2-SS-E3**) linker. This is likely due to protease cleavage being more efficient than disulfide cleavage (as opposed to increased retention due to the extra leucine residue) since protease-cleavable **Her2-VCL-R3** was also brighter than disulfide-linked **Her2-SSL-R3,** which gave a similar signal to disulfide conjugate **Her2-SS-R3**.

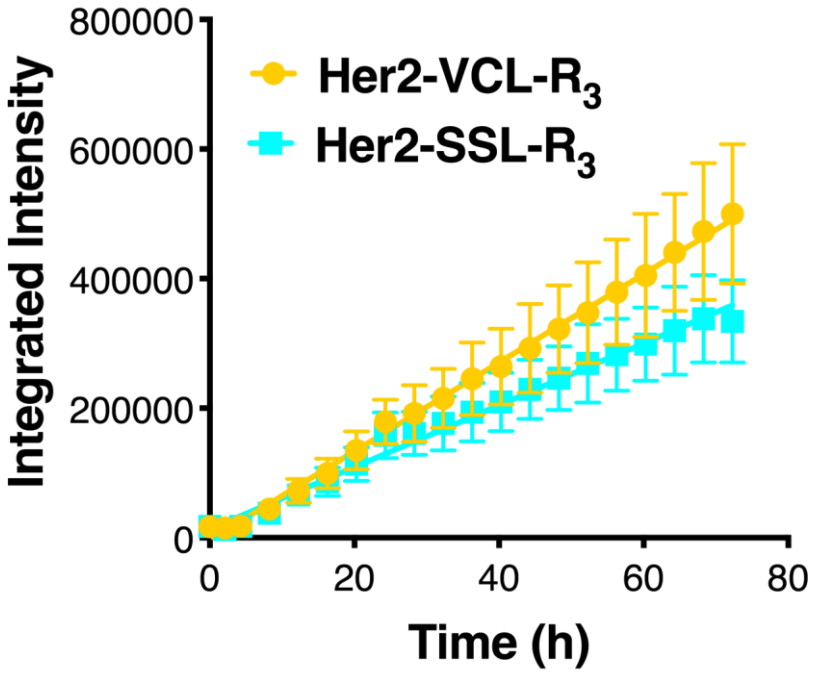

Figure S6. Disulfide probe is cleaved slightly less efficiently than peptide probe in cells. Incucyte kinetics of cleavage in SK-BR-3 cells for peptide-linked **Her2-VCL-R$_3$** and disulfide-linked **Her2-SSL-R$_3$** (designed to release the same catabolites upon respective cleavages) shows that slightly more BODIPY is released from the Val-Cit-Leu than disulfide linker.

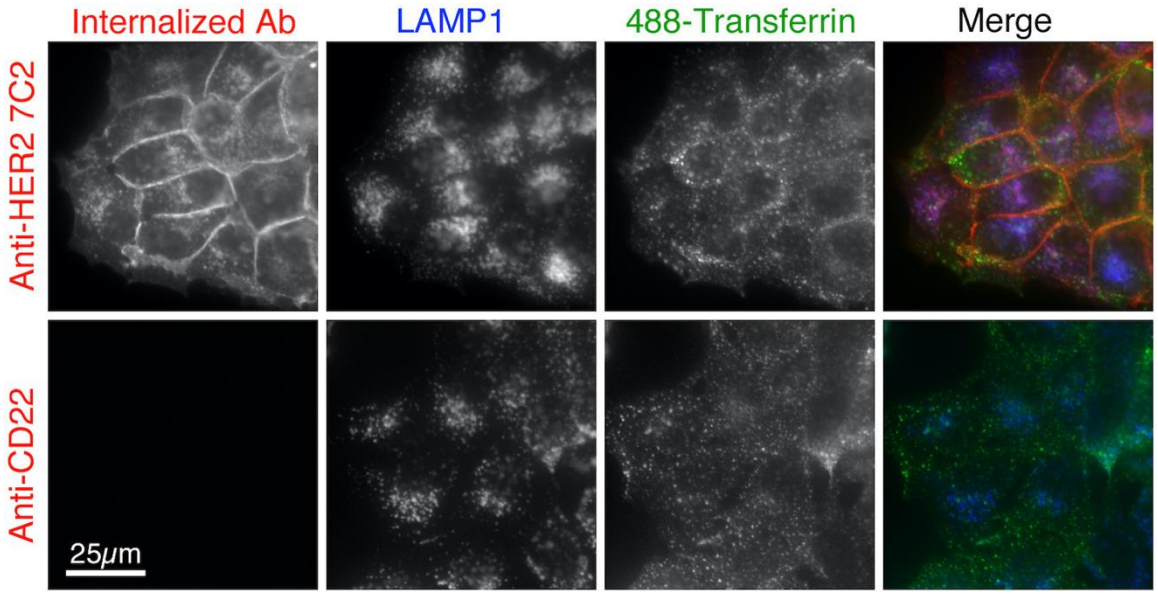

Figure S7. Unconjugated 7C2 accumulates in lysosomes overnight.
Unconjugated 7C2^{K149C} (upper panels) or anti-CD22 ^{K149C} non-binding control (lower panels) at 5 μg/ml were incubated for 19h with MCF-7/HER2 cells in the presence of lysosomal protease inhibitors to minimize degradation. During the last hour of incubation, 25 μg/ml Alexa488-transferrin (Molecular Probes T13342) was added to label the recycling pathway. Cells were then washed, PFA fixed, saponin permeabilized and stained with mouse anti-LAMP1 (BD Biosciences 555798 at 1:1000). Secondary antibodies, Cy3-anti-human and Alexa647 anti-mouse (Jackson Immunoresearch 709-166-149 and 715-606-150), were used at 1.9 μg/ml. Internal 7C2 (red channel) is mainly lysosomal at this time-point, since it colocalizes better with LAMP1 (blue channel, appearing magenta in the merged right panel) than with transferrin (green channel, with little yellow signal in the merge). As expected, non-targeting anti-CD22 was not detectable under these conditions, although the cells actively endocytosed Alexa488-transferrin. Scale bar is 25 μm.

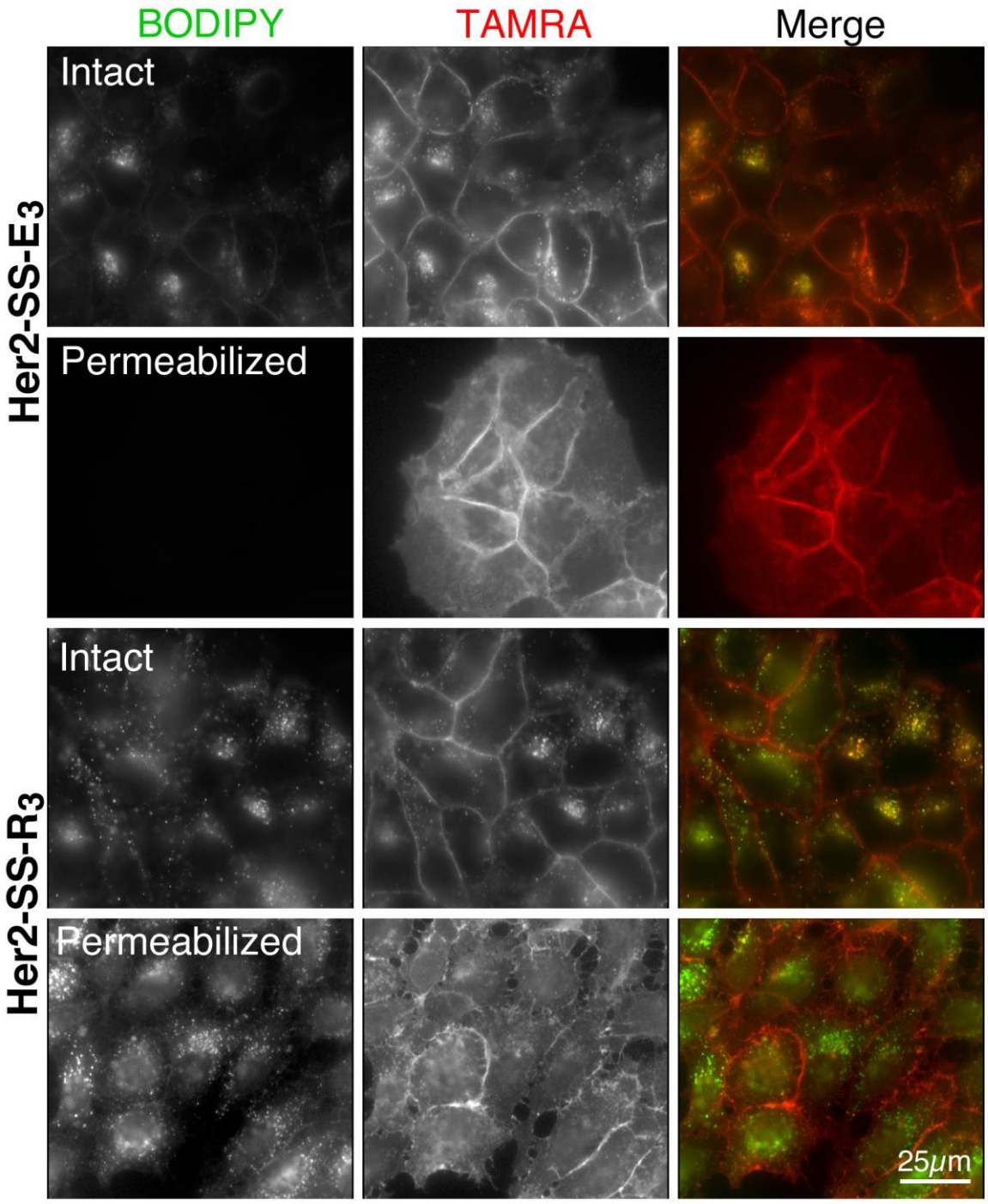

Figure S8. Catabolites released from Her2-SS-E$_3$ are not retained in lysosomes after saponin permeabilization. MCF-7/HER2 cells were incubated for 18.5h with **Her2-SS-E$_3$** (upper two rows) or **Her2-SS-R$_3$** (lower two rows), washed, fixed and treated with (Permeabilized) or without (Intact) saponin detergent prior to mounting. **Her2-SS-E$_3$** was exposed for 10x longer than **Her2-SS-R$_3$** in the BODIPY (but not TAMRA) channel to allow visualization of lysosomal BODIPY in intact cells, but this disappeared after permeabilization, suggesting negatively charged catabolites do not associate with the inner lysosomal membrane. By contrast, the positively charged dR$_3$-containing catabolites from **Her2-SS-R$_3$** reduction were at least partially retained in lysosomes after saponin treatment, as shown in **Figure 10**. Intracellular TAMRA was lost from permeabilized lysosomes with both conjugates.

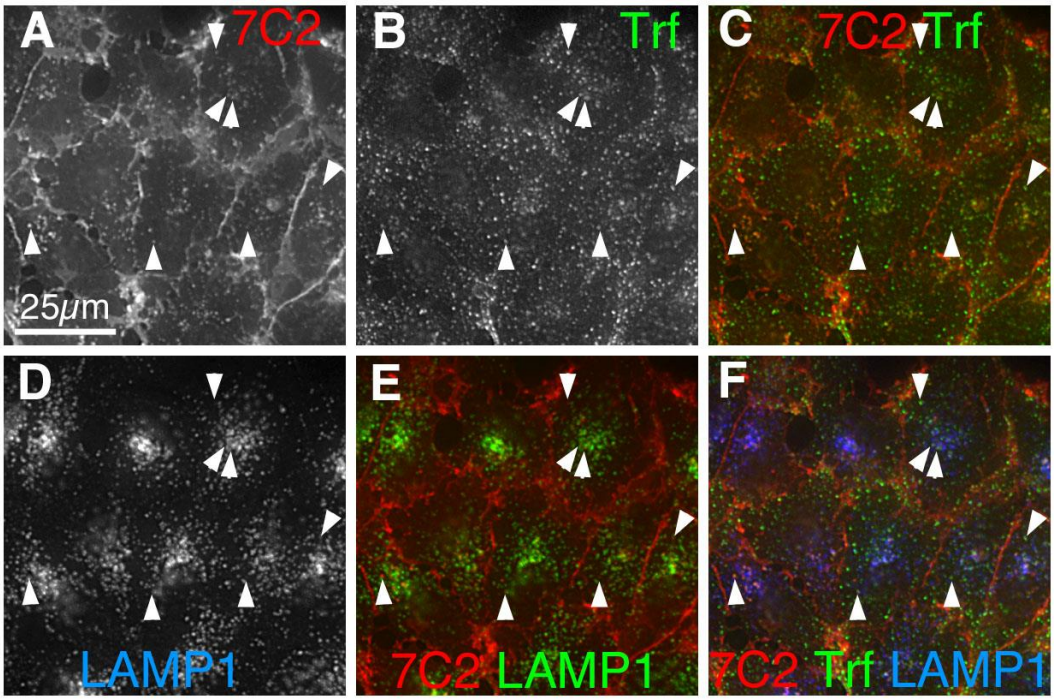

Figure S9. Unconjugated 7C2 is partially recycling after a 2h chase.
Unconjugated 7C2^{K149C} was bound to MCF-7/HER2 cells on ice for 1 h in carbonate-free medium containing 12.5μg/ml Alexa488-transferrin (Invitrogen T13342), washed and chased for 2 h in regular growth medium with fresh Alexa488-transferrin (green channel). Cells were then washed, PFA fixed, permeabilized with saponin and labeled for lysosomes with mouse anti-LAMP1 (1:1000 BD Biosciences 555798) followed by Alexa647 anti-mouse (1.88 μg/ml Jackson 715-606-150). LAMP1 is shown in the blue channel in the triple merge (F), but in the green channel in (E) to enable fairer comparison of the yellow merge with the transferrin overlay in (C). 7C2 was concurrently detected with Cy3-anti-human (1.88μg/ml Jackson 709-166-149) in the red channel in all merges. Scale bar is 25μm. Arrowheads indicate 7C2 in transferrin-positive endosomes.

Table S1. Analytical characterization (PAR, probe-to-antibody ratio; and % aggregate) of all HER2-targeted (and control CD22-targeted) FRET probes discussed in the main text.

Conjugate	PAR	% aggregate
Her2-SS	2.1	11
Her2-SS-R	2.2	1.9
Her2-SS-R_2	2.2	1.3
Her2-SS-R_3	2.0	0.65
Her2-SS-RE	1.6	2.2
Her2-SS-E	2.0	1.6
Her2-SS-E_2	2.2	1.1
Her2-SS-E_3	2.0	7.1
Her2-CC-R_3	2.0	1.7
Her2-VCL-R_3	2.0	2.5
Her2-VCL-E_3	2.0	2.7
Her2-VCL	2.0	2.8
Her2-SSL-R_3	2.0	2.8
CD22-SS-R_3	1.9	Not measured